Mechanisms of CO_2 Capture in Ionic Liquids: A Computational Perspective

Maxime Mercy,[a] Nora H. de Leeuw*[a,b] and Robert G. Bell*[a]

We present computational studies of CO_2 sorption in two different classes of ionic liquid. The addition of carbon dioxide to four superbase ionic liquids, [P3333][Benzim], [P3333][124Triz], [P3333][123Triz] and [P3333][Bentriz] was studied using DFT approach and considering anions alone and individual ion pairs. Addition of CO_2 to the anion alone clearly resulted in the formation of a covalently-bound carbamate function with the strength of binding correlated to experimental capacity. In the ion pair however the cation significantly alters the nature of the bonding such that the overall cohesive energy is reduced. Formation of a strong carbamate function occurs at the expense of weakening the interaction between anion and cation. In [N111][L-ALA], a representative amino acid ionic liquid, evidence was found for a low-enegy monomolecular mechanism for carbamate formation, explaining the 1:1 molar uptake ratio observed in some AAILs. The mechanism involves proton transfer to to the carboxylate group of the aminate anion.

Introduction

Ionic liquids have been widely investigated as potential carbon capture media since the first report of the solubility of CO_2 in [bmim][PF6] by Blanchard et al.[1] In addition to high capacities for CO_2 sorption, other favourable attributes of ionic liquids (IL) are their very low vapour pressures, high thermal stability and wide chemical tunability of both the cation and anion component. Many ionic liquids have subsequently been found to have promising CO_2 uptake and release capacities. The possibility of designing an IL specifically for CO_2 capture was first reported by Bates et al.[2], who used an amine functionalised anion to perform removal of CO_2 from natural gas. The maximum observed molar capacity of 0.5 CO_2/IL, together with other data indicating the formation of carbamate functions, suggested a bimolecular uptake mechanism, similar to that seen in neutral amines such as monoethanolamine where CO_2 chemisorption leads to the formation of an ion pair comprising a carbamate anion and an ammonium cation. In recent years there has been accelerating interest in functionalised ILs which can effect chemisorption of CO_2. This is associated with much higher capacities than physisorption, though it should be noted that strong binding of CO_2 is not necessarily advantageous if the adsorbing IL is subsequently required to be regenerated. In 2010, Wang and co-workers[3] reported 1:1 molar adsorption of CO_2 using an IL containing a so-called "superbase" (SB) or aprotic heterocyclic anion (AHA). A variety of SBILs were subsequently studied[4], with a link found between CO_2 uptake capacity and pK_a of the superbase anion. A range of functionalised ILs with superbase anions were discussed by Wu et al.[5], who investigated the relationship between adsorption enthalpy, calculated by first-principles methods, and observed CO_2 capacity with the aim of designing Ils optimised for the CO_2 capture process. They also drew attention to the problem of viscosity, which tends to increase with CO_2 content in many amine-functionalised ILs, but far less so with may aprotic anions. In 2015, Taylor and co-workers[6] measured the CO_2 adsorption capacities for a range of SBILs under wet and dry conditions. Among four SBILs, based on N-heterocyclic aprotic anions, molar adsorption capacities ranged from 30% to 120%. ^{13}C-NMR spectroscopy confirmed the formation of carbamate bonds during the capture process.

Ionic Liquids based on amino acids (AAILs), where the anion is an aminate, has also been proposed as potential CO_2 capture media, due to their possession of an amino group on the anion. A number of authors[7-10] have studied CO_2 adsorption in AAILs. The molar uptake ratio can be 1:1 or 1:2 molar depending on the anion and the cation. For example $[N_{2224}]$[ALA] shows an absorption capacity of 1 mole of CO_2 for 2 moles of ionic liquids (1:2), typical of amino-funtionalised ILs, whereas $[P_{666,14}]$[PRO] exhibits equimolar absorption (1:1) [9]. The question arises then as to whether two different mechanisms are in operation. A maximum 1:2 ratio implies the classic bimolecular amine mechanism; 1:1 suggests a monomolecular mechanism involving one anion, possibly terminating at the formation of carbamic acid group on the anion. It is commonly known that amino acids in solution form a stable zwitterion by transfer of the acidic proton to the amine resulting in a combination of a carboxylate and an ammonium. The anion derived from an amino acid is the basic form composed of a carboxylate and a primary amine. However upon chemisorption of CO_2, a shift of proton to the original carboxylate function could also be imagined. Equally it is possible that a monomolecular mechanism is more broadly dominant with dimerization occurring subsequently. Recently[8], a combination of NMR and IR-spectroscopy suggests an intramolecular carbamate mechanism to explain the 1:1 mechanism with post-dimerization being proposed to explain observation of the 1:2 capacity.

In this paper we examine computationally two aspects of CO_2 capture in ionic liquids. In the first part we review a study of ionic liquids based on the so-called "superbase" or aprotic heterocyclic anion. Four different anions are studied, and it is shown that the enthalpy of sorption of CO_2on the anion is strongly related to the experimental CO_2 capacity. Inclusion of a cation in the calculations illustrates that CO_2 binding acts to weaken the interionic forces within the IL. In the second part we introduce a DFT study of CO_2 addition to a model amino acid IL. Again, anion-only and ion pair models are used. We show that a monomolecular mechanism is energetically feasible, leading to 1:1 molar uptake of CO_2.

Methodology.

Density functional theory calculations were carried out using the Minnesota density functional M06[11]. This hybrid meta-exchange correlation functional is versatile and included in its construction is a non-local interaction term that make it well-suited to the treatment of ionic and hydrogen bonding[12]. Its predecessor M05 has been tested successfully for ionic liquids[13]. A Pople basis set 6-311+G(d,p) was used for all atoms. All cations, anions and ionic pairs were optimised using the software Gaussian 09[14] without symmetry constraints and, for each geometry, the nature of minima were checked with a frequency calculation. Energies were corrected for the zero-point energy and relative enthalpies were calculated at 298.15 K. Natural bond analysis (NBO) was carried out with NBO 3.1[15] as implemented in Gaussian 09. Atoms in Molecules (AIM) analysis[16] was done with multiwfn[17]. For each ion pair, there are multiple possibilities to arrange the cation and the anion to form each ionic pair. For the SBILS, two methods of building ionic pairs were followed in order to obtain local minima near to the global minimum on the potential energy surface. In the first, a molecular dynamics trajectory of five ns was generated at high temperature in the NVT ensemble using the AMBER software with the GAFF force field[18]. A large cell with one ionic pair was used. From the resulting trajectory, ten to twenty steps were extracted. These structures were optimized at DFT level with a small basis set, and the five most stable structure were then optimized at the M06/6-311+G(d,p) level. In parallel, the tetraalkylphosphonium cation and the anion were positioned in different configurations by human chemical intuition and optimized. For each SBIL ion pair, multiple minima were found which were very close in energy to the most favourable structure. This can be attributed to the configurational flexibility of the cation's alkyl chains. In the following analyses, only the most favourable structures are described. The geometries were created and monitored with Molden[19] and VMD[20].

2 Results and Discussion

A Superbase ionic liquids

The ion pair

Minimum energy ion pair configurations are shown in figure 1 and the pairing energies are given in table 1, along with data on the amount of charge transfer between cation and anion, and the shortest interionic N-P distance. From figure 1 it can be discerned that in general the cation and anion are positioned relative to one another so as to maximise the interactions between heterocyclic nitrogen and the H_{C1} hydrogens, i.e. those bonded directly to the α-carbons of the phosphonium ion. N-H_{C1} distances are shown where they are less than 2.75 Å. The ascending order of pairing strength is [Benzim] < [Bentriz] < [124Triz] < [123Triz]. In fact there is a rough correlation between the pairing energy and the number of N-H_{C1} distances less than 2.75 Å, namely 3, 5, 7 and 8 respectively, though considering only the shortest such distance, there is no correlation with the pairing energy. For [124triz], the configuration of the three nitrogen atoms means that one of the aromatic nitrogens, N_4, must point away from the phosphonium cation. For [Bentriz] the three adjacent nitrogens intract strongly with the cation such that the benzene ring is effectively a spectator. By contrast, [Benzim] shows a π-H_{C1} interaction with its benzene ring, which affords additional stability to the ionic pair. In all the cases, of course, additional van der Waals interactions are likely to exist with longer chain cations, and within the bulk liquid. In a previous work [21], we carried out a detailed analysis of the bonding using NBO[15]. Key findings were that that the interionic bonding may be characterised in terms of a manifold of weak bonds, involving nitrogen as a lone pair donor, interacting with an empty σ bond orbital, either σ* (C-H) or σ* (P-C). An analysis using Bader's Atoms in Molecules (AIM) approach[16] suggested that none of these hydrogen bonds had a strength greater than 16 kJ mol^{-1}. Charge distribution analysis was carried also out using AIM, and the overall charge transfer from anion to cation is summarised in table 1. The values of charge transfer lie between 0.06 and 0.12. Again this quantity is correlated to the pairing energy, with stronger pairing being characterised by a larger charge transfer.

Table 1. Selected properties of the ionic pairs. ΔE_{IP}: pairing energy of the ionic pair. δ_{anion} is the sum of the NAO charges on the anion. CT = 1-$|\delta_{anion}|$ corresponds to the charge transfer from the anion to the cation. r_{SN} is the shortest distance between nitrogen and the cation phosphorus.

	Ionic Pair	ΔE_{IP} /kJ mol^{-1}	δ_{anion}	CT	r_{SN} /Å
a	[P_{3333}][Benzim]	-363.25	-0.94	0.06	2.19
b	[P_{3333}][124Triz]	-374.50	-0.92	0.08	2.16
c	[P_{3333}][123Triz]	-396.59	-0.88	0.12	2.26
d	[P_{3333}][Bentriz]	-371.74	-0.93	0.07	2.25

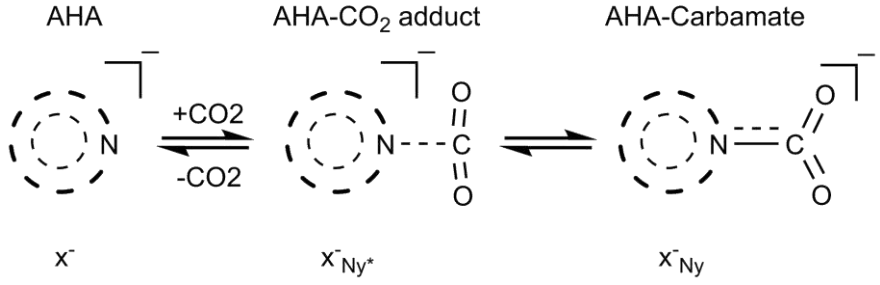

Scheme 1. Representation of the adduct, X^-_{Ny*}, and carbamate product, X^-_{Ny}, from CO_2 addition on a nitrogen Ny of an N-heteroaromatic anion (AHA), X^-

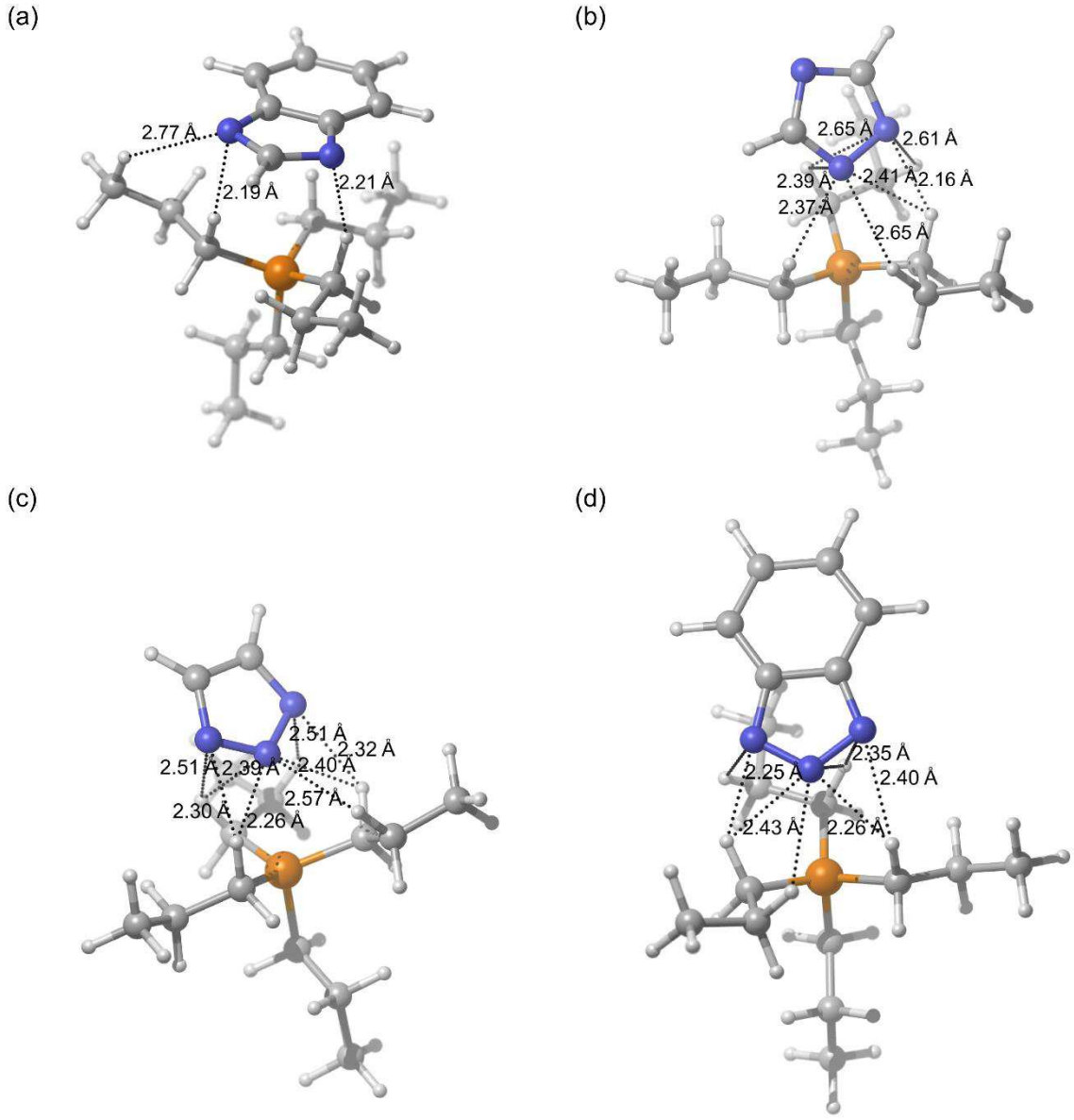

Figure 1. Ionic pairs comprising a tetrapropylphosphonium cation, $[P_{3333}]^+$, with the four anions: (a) $[P_{3333}]$[Benzim], (b) $[P_{3333}]$[124Triz], (c) $[P_{3333}]$[123Triz] and (d) $[P_{3333}]$[Bentriz]. Dashed lines indicate intermolecular N-H distances less than or close to the sum of the vdW radii (2.75 Å) Colour code: blue – nitrogen; yellow – phosphorus; grey – carbon; white – hydrogen.

Interaction with CO_2.

The addition of CO_2 was investigated assuming the mode of binding shown in Scheme 1, i.e. with bonding principally only to nitrogen atoms of the anion. There are two distinct cases encountered: chemisorption of CO_2 resulting in N-C carbamate bond formation and loss of CO_2 linearity, and an intermediate "adduct" state in which CO_2 is closely physisorbed but no covalent bond formation occurs. In our current SBIL systems[21], we observe both these types of CO_2 binding, which occur as minima on the potential energy surface.

Addition of CO_2 to Superbase Anion

Addition of CO_2 to the anion only was attempted at all non-equivalent nitrogen positions of the four anions. Related data are given in table 2. There are a number of key points to observe. In all cases, chemisorption of CO_2 is exothermic, but despite the similarity between the four anions, which all coordinate to CO_2 through aromatic N atoms, the energies of addition vary considerably between -13 kJ mol^{-1} and -56 kJ mol^{-1}. Even the lowest energy configurations for each anion vary between -30 and -56 kJ mol^{-1}. Importantly we also see here a clear correlation between the experimentally observed CO_2 uptake and the value of the carbamate formation enthalpy, namely the sequence $[Bentriz]^-$ < $[123Triz]^-$ < $[124Triz]^-$ < $[Benzim]^-$. The correlation between the two quantities can be clearly seen in figure 2 where we also show analogous energies calculated by other authors. [4, 22] From table 2(b) we also note the energies of the physisorbed adduct, where located, are generally lower than for the carbamate. However for $[Bentriz]^-$ and $[123Triz]^-$ energies are within a few kJ mol^{-1}, and for $[Bentriz]^-_{N2}$ the adduct is even energetically preferred.

Table 2. Selected properties for (a) carbamate formation for the anion alone $\mathbf{x}^-_{Ny}$ and (b) the respective adduct formation $\mathbf{x}^-_{Ny*}$. nl=not located on the PES

(a)	ΔH_r /kJ mol^{-1}	d(Nx-C) /Å	α(OCO) /º	|θ| /º	δ'_{AHA}	δ'_{CO2}	(b)	ΔH_a /kJ mol^{-1}	d(Nx-C) /Å	α(OCO) /º
[Benzim]$^-_{N1}$	-55.99	1.55	136.1	179.8	-0.46	-0.54	**[Benzim]$^-_{N1*}$**	-30.81	2.39	165.4
[124Triz]$^-_{N1}$	-55.24	1.59	137.9	179.9	-0.46	-0.54	**[124Triz]$^-_{N1*}$**	nl		
[124Triz]$^-_{N4}$	-54.29	1.57	137.1	180.0			**[124Triz]$^-_{N4*}$**	nl		
[123Triz]$^-_{N1}$	-47.60	1.61	138.6	179.9	-0.51	-0.49	**[123Triz]$^-_{N1*}$**	nl		
[123Triz]$^-_{N2}$	-38.44	1.67	140.5	179.7			**[123Triz]$^-_{N2*}$**	-31.35	2.32	163.3
[Bentriz]$^-_{N1}$	-30.80	1.62	138.8	179.9	-0.53	-0.47	**[Bentriz]$^-_{N1*}$**	-26.03	2.47	168.1
[Bentriz]$^-_{N2}$	-13.54	1.82	146.3	179.5			**[Bentriz]$^-_{N2*}$**	-23.71	2.52	169.1

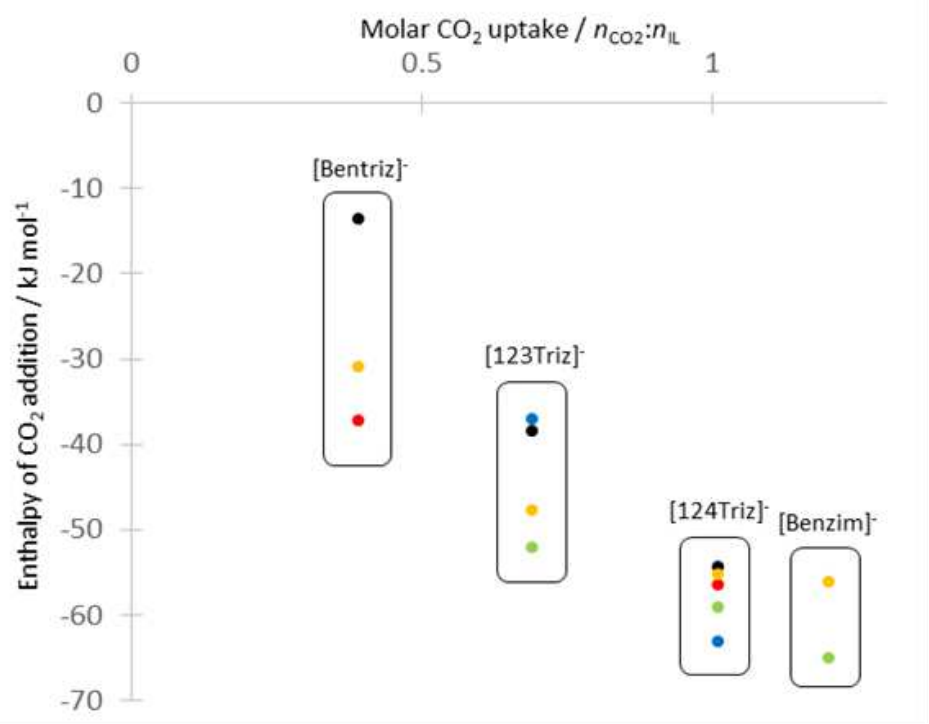

Figure 2. Comparison of calculated CO_2 addition enthalpies for the four anions from the anion-only model, plotted against experimental CO_2 uptake from Taylor et al. Key to data points: red circles from Wang et al. for $[124Triz]^-_{N4}$ and $[Bentriz]^-_{N4}$, green from Seo et al. for x^-_{N1}, blue from Seo et al. for $[124Triz]^-_{N4}$ and $[123Triz]^-_{N2}$, yellow and black from this work for x^-_{N1} and x^-_{N2} respectively.

Addition of CO_2 to the Ion Pair

The formation of carbamate and CO_2 adducts on a single ion pair, comprising a superbase anion and $[P_{3333}]^+$ cation was also simulated. As in the case of the anion, all non-equivalent N positions were considered. The calculated energies are given in table 3. The enthalpies of reaction and adduct formation, ΔH_r and ΔH_a respectively, are calculated with reference to the separate CO_2 and optimised ion pair, i.e. differences in pairing strength are not reflected in the ΔH values. For each of the ion pairs, the carbamate formation energy is clearly less favourable that that for the anion alone, and is even endothermic at some nitrogen positions ($[123Triz]_{N2}$ and $[Bentriz]_{N2}$) as a result of including the cation in the calculation. We also see that relationship with the experimental adsorption capacity is less clearly defined. With the lowest values of ΔH for each ion pair [Benzim] and [124Triz] are the most strongly bound and [123Triz] and [Bentriz] the least. In the latter two cases, the order is reversed from the experimental trend. It is clear that, for these ion pairs, the adducts fall in the same energy range as the carbamate products, indicating possible competition between physi- and chemisorption. In order to gain more insight into the energetics and bonding of CO_2 within the

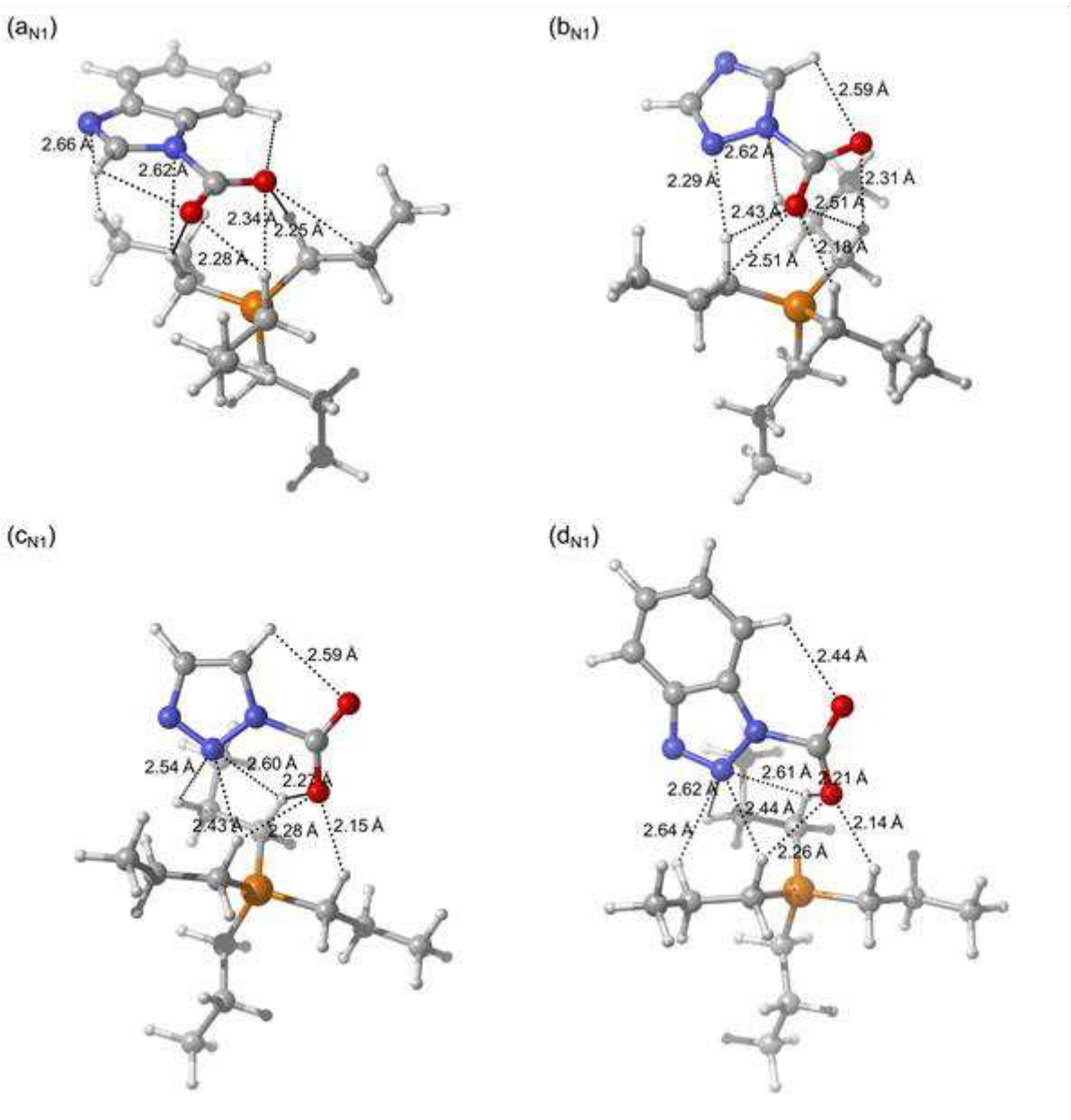

Figure 3. Carbamate ionic pairs resulting from N_1 CO_2 addition on the four ionic pairs: (a) $[P_{3333}]$[Benzim], (b) $[P_{3333}]$[124Triz], (c) $[P_{3333}]$[123Triz] and (d) $[P_{3333}]$[Bentriz]. Dashed lines indicate intermolecular N···H or O···H distances less than or close to the sum of the vdW radii (2.75 Å) Colour code: blue – nitrogen; yellow – phosphorus; grey – carbon; white – hydrogen, red - oxygen.

Table 3. Selected properties for (a) carbamate formation on the ionic pair $[P_{3333}][\mathbf{x}]$ for each nitrogen Ny on the anion **x** ($\mathbf{x}_{Ny}$) and (b) the respective adduct formation $\mathbf{x}_{Ny}$*. nl=adduct not located on the PES

(a)	ΔH_r /kJ mol^{-1}	d(Nx-C) /Å	α(OCO) /°	|θ|(CNCO) /°
[Benzim]$_{N1}$	-35.82	1.49	131.5	3.7
[124Triz]$_{N1}$	-32.62	1.51	133.6	8.4
[124Triz]$_{N4}$	-9.06	1.49	131.9	6.4
[123Triz]$_{N1}$	-13.50	1.57	137.0	3.5
[123Triz]$_{N2}$	+1.91	1.52	132.9	7.8
[Bentriz]$_{N1}$	-13.03	1.55	136.0	4.0
[Bentriz]$_{N2}$	+14.47	1.62	138.0	17.2

(b)	ΔH_a /kJ mol^{-1}	d(Nx-C) /Å	α(OCO) /°
[Benzim]$_{N1*}$	-8.29	2.61	172.2
[124Triz]$_{N1*}$	-21.92	2.79	175.3
[124Triz]$_{N4*}$	-17.93	2.77	175.1
[123Triz]$_{N1*}$	-12.46	2.70	174.2
[123Triz]$_{N2*}$	nl		
[Bentriz]$_{N1*}$	-10.63	2.74	174.5
[Bentriz]$_{N2*}$	-15.66	2.79	176.0

ion par, an ion paring energy ΔE_{IPCO2} was determined for each of the ion pair-carbamate products. This energy was defined with respect to the optimised anion-only carbamate and separate optimised $[P_{3333}]^+$ cation. These data are given in table 4, together with characteristic distances and values extracted from NAO charge analyses of the optimised ion pair-carbamate clusters. For each ion pair, ΔE_{IPCO2} was more negative in the case where the carbamate binding was stronger. However in general, the difference in ion pairing energies before and after carbamate formation is broadly similar to the difference between the carbamate formation energy in the anion-only and ion pair models:

$$\Delta H_r(\mathbf{x}_{Ny}) - \Delta H_r(\mathbf{x}^-_{Ny}) =\sim (\Delta E_{IPCO2}-\Delta E_{IP})$$

In other words, formation of a carbamate function by adsorption of CO_2 always has a corresponding destabilising effect on the bonding between the cation and anion, which partly explains why there can be a fine balance between physi- and chemisorption, as observed for the [123Triz] and [Bentriz] ionic pairs. For these ion pairs, an equilibrium between coordinated and non-coordinated CO_2 could plausibly exist, explaining the lower experimental CO_2 uptake. By contrast, the strong preference for N_1-carbamate formation for [Benzim] and [124Triz] is consistent with the observed high CO_2:IL molar ratio, suggesting possible 1:1 uptake via (virtually complete) carbamate formation.

In terms of the geometries of the optimised systems (fig. 3) the effect of CO_2 addition can be seen in shifts in the relative positions of anion and cation. The superbase aromatic component moves away from its optimum position, allowing closer interaction between the COO^- moiety and the cation. This can be quantified, for instance in the case of $[P_{3333}]$[Benzim], by the r_{SN} distance increasing from 2.19 Å (without CO_2) to 2.62 Å, whereas the shortest O_{COO-}-H_{C1} distance is 2.25 Å. The important network of weak interionic hydrogen bonds involving aromatic nitrogen is significantly disrupted, due to the preferential binding to CO_2. By contrast, in the adducts [PCCP] the position of the anion is less affected by the presence of CO_2.

As seen previously for the anion, the bonding strength of carbamate can be characterised by its geometric properties (table 3): the N_x-C carbamate bonds are generally shorter in the ion pair than for the anion-only model, and the O-C-O angles are also lower. Thus it seems that, although overall ΔH_r values are less favourable in the ionic pair, the bonding of the carbamate moiety itself is actually stronger. There are two things which should be noted here; firstly the presence of the cation increases the negative charge on the N_1 nitrogen for [124Triz], [123Triz] and [Bentriz] thereby enhancing the Lewis basicity at that position. Secondly the overall charge distribution between the superbase ("original" anion) and CO_2 moieties shows distinct changes: in the anion-only model about half the negative charge of the anion is transferred to the CO_2 (δ'_{CO2} in table 2). In the ion pair-carbamate, the overall charge transfer (see table 4) between anion and cation is similar to the case without CO_2 present, but virtually all the charge transfer is from the superbase (AHA), making the anion less negative overall, with the exception of the carbamate (NCOO) function. The combined effect is thus that the cation has a significant effect of strengthening the carbamate bond while at the same time weakening the anion-cation interaction. The extent to which this occurs also depends significantly on the anion.

Table 4. Selected properties of the most stable ionic pair-carbamates Charges δ from NAO analysis of the carbamate with δ'_{AHA} and δ'_{CO2} the NAO charges as split between the superbase and CO_2 moieties. r_{SN} and r_{SO} are respectively the shortest distances between N(anion) and H(cation) and between O(carbamate) and H(cation).

	ΔE_{IPCO2} /kJ mol^{-1}	δ'_{AHA}	δ'_{CO2}	CT	r_{SN} /Å	r_{SO} /Å
[Benzim]$_{N1}$	-344.18	-0.35	-0.59	0.06	2.62	2.25
[124Triz]$_{N1}$	-351.68	-0.38	-0.55	0.08	2.29	2.18
[124Triz]$_{N4}$	-328.37	-0.37	-0.55	0.07		
[123Triz]$_{N1}$	-363.09	-0.45	-0.50	0.05	2.43	2.15
[123Triz]$_{N2}$	-356.22	-0.38	-0.55	0.07		
[Bentriz]$_{N1}$	-354.17	-0.43	-0.52	0.05	2.44	2.14
[Bentriz]$_{N2}$	-340.58	-0.50	-0.46	0.04		

B Amino Acid ionic liquids

As a representative of ionic liquids based on aminate anions, we report results on the ion pair $[N_{1111}][ALA]$. This has been used as an initial model system to explore possible mechanisms for CO_2 uptake in such AAILs. The alanate ion derived from the biologically-common L-alanine enantiomer was chosen, though for convenience we refer to the anion as $[ALA]^-$. As discussed earlier, a 1:2 CO_2:IL molar uptake ratio, as commonly observed in many cases, implies a bimolecular mechanism, analogous to that observed for organic amines, wherein CO_2 forms a carbamate bond, with a proton transferring to a second amine molecule to form an ammonium-carbamate pair. An alternative 1:1 ratio suggests an intramolecular mechanism, with each anion accommodating one CO_2. Evidence strongly suggests that this would be solely via carbamate (or carbamic acid) formation. In terms of chemisorption of CO_2, alternative competing monomolecular and bimolecular mechanisms may therefore exist depending on the precise nature of the ion pair, and also potentially on other conditions. It should also be noted that a favourable monomolecular mechanism for initial CO_2 uptake does not preclude subsequent dimerization, leading to the observation of a 1:2 uptake capacity. For this reason we have initially studied the energetics of intramolecular CO_2 addition mechanisms. Local minina and transition states for the possible pathways have been calculated using both anion-only and ion pair models.

Intramolecular pathway

The addition of CO_2 was investigated according to the possible intramolecular mechanisms shown in scheme 2. In pathway (i), CO_2 addition to the amine function, forming a carbamate bond is accompanied by proton shift from the original amino group to the carboxylate function, resulting in the formal negative charge now residing on the carbamate. We refer to this as the carbamate or "*carba*" mechanism. Conversely in pathway (ii) the proton shifts onto the newly-bound CO_2 moeiety, forming carbamic acid, with the anionc carboxylate retained. In the present work this is denoted as the "*carbo*" mechanism. Ultimately the anion may achieve the 7-membered ring structure shown as $\mathbf{b}_3^-$. However, it can be imagined that the two separate pathways via $\mathbf{b}_1^-$ or $\mathbf{b}_2^-$ could have very different energetics, which may also depend on the nature of other ions in the immediate proximity.

In table 5 the energies of species involved in the mechanisms are given. Both ΔE corrected for zero-point energy (ΔE^{ZPE}) and ΔH at 298 K are given for comparison. The species are denoted as in scheme 2, and also include adducts, a^---CO_2, which are found by following the intrinsic reaction coordinate. Species from the ion pair model are illustrated in fig. 4.

In the *carba* pathway, (i), the addition of CO_2 to the anion nitrogen N_a leads to a 5-membered ring transition

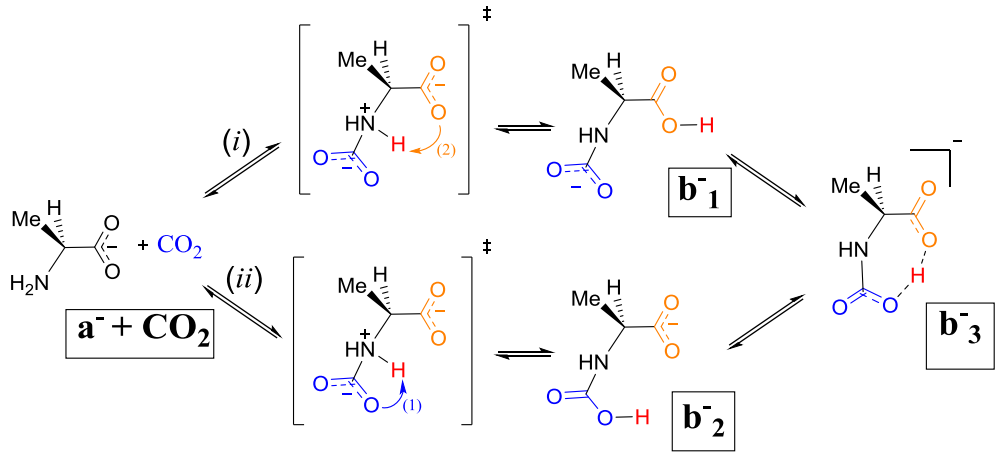

Scheme 2. Possible intramolecular pathways for binding of CO_2 to the $[L\text{-}Ala]^-$ anion.

state (Fig. 4). An N-H bond is broken whereas an O-H bond is formed; a proton is thus transferred from the amine group to the carboxylate to form $\mathbf{b^-_1}$, a bifunctional anion with carboxylic acid and carbamate groups. In the *carbo* pathway, (ii), the addition of CO_2 on the anion nitrogen N_a leads to a 4-membered-ring transition state TS(ii) (x). In this case a hydrogen is transferred from the amine group to the carbamate to form $\mathbf{b^-_2}$, an anion with carbamic acid and carboxylate function. Thermodynamically, the two products are in competition as the energy difference between products $\mathbf{b^-_1}$ and $\mathbf{b^-_2}$ is less than 10 kJ mol^{-1} for both the anion-only and ion pair model, though the presence of the cation makes the $\mathbf{b^-_2}$ very slightly exothermic with respect to the ion pair and CO_2 separately. However a major difference between the pathways is the accessibility of the transition state: TS(i) is always much more favourable that TS(ii), by about ~80-90 kJ mol^{-1}, implying that the *carba* mechanism would dominate under normal conditions. A simple explanation is that *carbo* mechanism will always require a 4-membered ring transition state, which is intrinsically more strained that a 5-membered ring.

Finally, from both products, it is possible to locate a common post-product $\mathbf{b^-_3}$. It is obtained by the rotation of the anion's CO_2 groups about their N-C bonds resulting in the proton being shared between the two carboxylate functions. $\mathbf{b^-_3}$ is close to, or lower in energy than $\mathbf{b^-_1}$ and $\mathbf{b^-_2}$, and the energetic barriers to bond rotation are not especially large, making interconversion possible between the three products $\mathbf{b^-_1}$, $\mathbf{b^-_2}$ and $\mathbf{b^-_3}$.

Table 5. Calculated energies of species from intramolecular pathways (i) and (ii) for addition of CO_2 to $[N_{1111}][ALA]$, ion both the anion-only and ion pair models. All energies in kJ.mol^{-1}.

		(i) ***carba***			(ii) ***carbo***			
		a^---CO_2	TS(i)	b^-_1	a^---CO_2	TS(ii)	b^-_2	b^-_3
$[ALA]^-$	ΔE^{ZPE}	-17.95	-1.72	-20.80	-26.53	94.33	-28.44	-63.75
	ΔH	-21.00	-6.87	-25.35	-29.67	89.50	-31.67	-69.45
IP	ΔE^{ZPE}	-17.27	30.80	-4.06	-20.13	126.19	5.37	-18.80
	ΔH	-20.23	24.20	-9.50	-22.47	120.48	0.66	-23.32

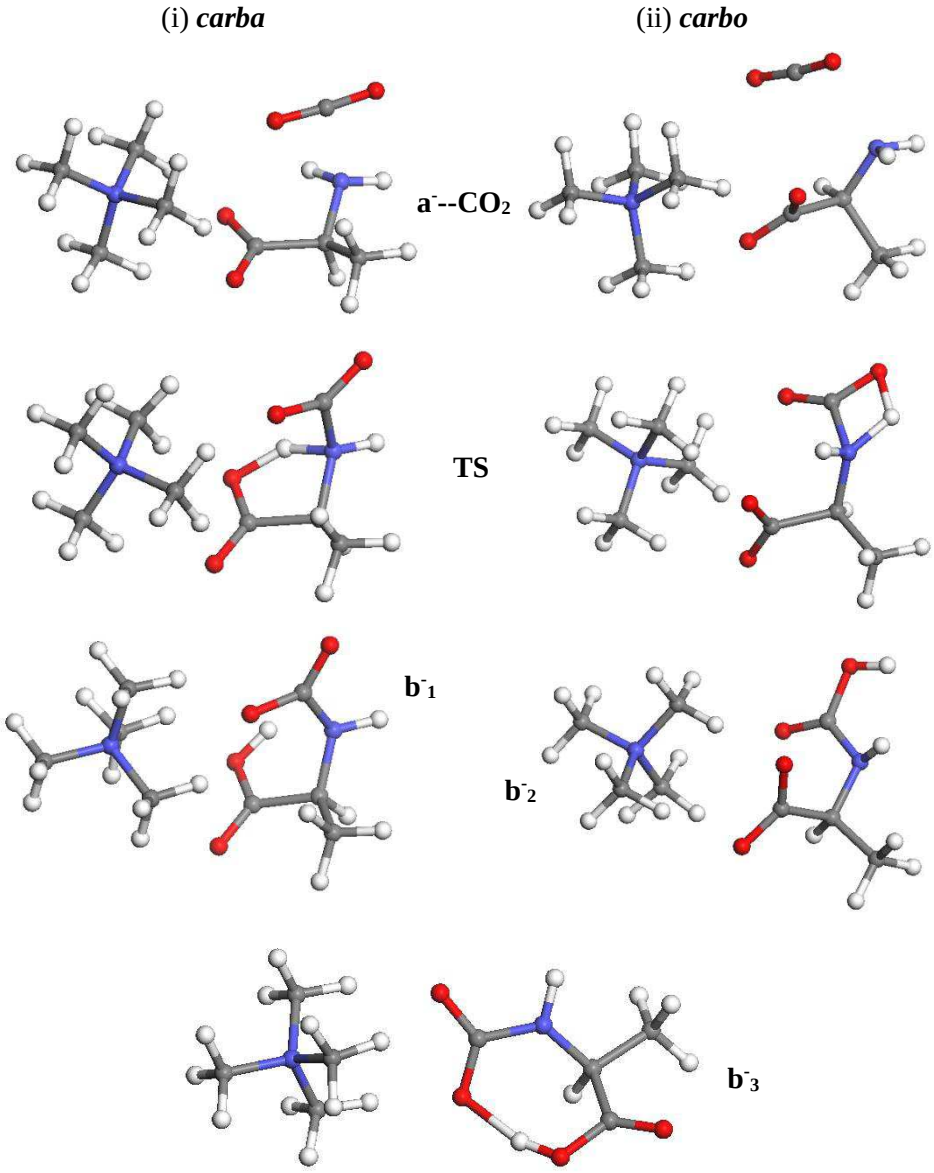

Figure 4. Molecular species from the two intramolecular pathways for CO_2 addition to $[N_{1111}][ALA]$ in the ion pair model. All species labelled as in Scheme 2.

Conclusions

In this work we have examined mechanisms of CO_2 uptake in two different classes of ionic liquid, with the aim of elucidating aspects of the adsorption process which may lead to the design of more effective IL sorbents. It is clear from both experiment and computation that functionalised anions containing classic amino groups, or aprotic heterocyclic N-donors, will always tend to bond strongly via carbamate bond formation (chemisorption). In order to maximise the CO_2 uptake in such ILs, the overall enthalpy of sorption needs to be optimised. This can include a significant counteracting contribution arising from the weakening of the interionic bonding. In the superbase ILs studied, the enthalpy was most strongly influenced by the basicity of the N-donor, depending on the number of neighbouring N atoms in the 5-membered aromatic ring. On the other hand, it may not always be desirable to have the strongest binding: requirements of sorbent regeneration may dictate the use of ILs with intermediate capacity for CO_2. In this regard, in would be beneficial to consider ILs in which carbamate formation occurs, but is less exothermic, and an equilibrium

can be established between physi- and chemisorbed species. In the case of the SBILs studied, this occurs when the ionic hydrogen bond network is disrupted by CO_2 sorption.
The study of the amino acid IL $[N_{1111}][ALA]$ revealed the existence of a thermodynamically feasible monomolecular mechanism for carbamate formation, which accounts for the 1:1 molar CO_2 uptake capacity observed for some AAILs. A mechanism involving proton transfer to the (non N-bonded) carboxylate group is strongly favoured since the alternative proton transfer to the carbamate involves a more strained 4-membered ring transition state. However the "carbamate" and "carboxylate" are closer in energy that the transition states. From experimental studies it is clear that a wide range of uptake capacities is possible in AAILs, depending on the identity of the anion as well as the cation, which again suggest that the AAIL could be "tuned" to target an optimal CO_2 capacity. Further studies will be required in order to compare the monomolecular with bimolecular mechanisms, and to consider the effect of different aminate anions on the CO_2 addition process.

Acknowledgements

This work was carried out as part of the "4CU" programme grant, aimed at sustainable conversion of carbon dioxide into fuels, led by the University of Sheffield and carried out in collaboration with the University of Manchester; Queen's University Belfast; and University College London. The authors therefore gratefully acknowledge the Engineering and Physical Sciences Research Council (EPSRC) for supporting this work financially (Grant No EP/K001329/1). The authors also acknowledge the use of the UCL Legion High Performance Computing Facility (Legion@UCL), and associated support services, in the completion of this work

References

1. L. A. Blanchard, D. Hancu, E. J. Beckman and J. F. Brennecke, *Nature*, 1999, **399**, 28-29.
2. E. D. Bates, R. D. Mayton, I. Ntai and J. H. Davis, *J. Am. Chem. Soc.*, 2002, **124**, 926-927.
3. C. Wang, H. Luo, D.-e. Jiang, H. Li and S. Dai, *Angew. Chem. Int. Ed.*, 2010, **49**, 5978-5981.
4. C. Wang, X. Luo, H. Luo, D.-e. Jiang, H. Li and S. Dai, *Angew. Chem. Int. Ed.*, 2011, **50**, 4918-4922.
5. C. Wu, T. P. Senftle and W. F. Schneider, *PCCP*, 2012, **14**, 13163-13170.
6. S. F. R. Taylor, C. McCrellis, C. McStay, J. Jacquemin, C. Hardacre, M. Mercy, R. G. Bell and N. H. de Leeuw, *J. Solution Chem.*, 2015, **44**, 511-527.
7. B. F. Goodrich, J. C. de la Fuente, B. E. Gurkan, D. J. Zadigian, E. A. Price, Y. Huang and J. F. Brennecke, *Ind. Eng. Chem. Res.*, 2011, **50**, 111-118.
8. Y. S. Sistla and A. Khanna, *Chemical Engineering Journal*, 2015, **273**, 268-276.
9. B. E. Gurkan, J. C. de la Fuente, E. M. Mindrup, L. E. Ficke, B. F. Goodrich, E. A. Price, W. F. Schneider and J. F. Brennecke, *J. Am. Chem. Soc.*, 2010, **132**, 2116-2117.
10. J. W. Ma, Z. Zhou, F. Zhang, C. G. Fang, Y. T. Wu, Z. B. Zhang and A. M. Li, *Environ. Sci. Technol.*, 2011, **45**, 10627-10633.
11. Y. Zhao and D. G. Truhlar, *Theor. Chem. Acc.*, 2008, **120**, 215-241.
12. M. Walker, A. J. A. Harvey, A. Sen and C. E. H. Dessent, *J. Phys. Chem. A*, 2013, **117**, 12590-12600.
13. E. I. Izgorodina, U. L. Bernard and D. R. MacFarlane, *J. Phys. Chem. A*, 2009, **113**, 7064-7072.
14. M. J. Frisch, G. W. Trucks, H. B. Schlegel, G. E. Scuseria, M. A. Robb, J. R. Cheeseman, G. Scalmani, V. Barone, B. Mennucci, G. A. Petersson, H. Nakatsuji, M. Caricato, X. Li, H. P. Hratchian, A. F. Izmaylov, J. Bloino, G. Zheng, J. L. Sonnenberg, M. Hada, M. Ehara, K. Toyota, R. Fukuda, J. Hasegawa, M. Ishida, T. Nakajima, Y. Honda, O. Kitao, H. Nakai, T. Vreven, J. A. Montgomery Jr., J. E. Peralta, F. Ogliaro, M. J. Bearpark, J. Heyd, E. N. Brothers, K. N. Kudin, V. N. Staroverov, R. Kobayashi, J. Normand, K. Raghavachari, A. P. Rendell, J. C. Burant, S. S. Iyengar, J. Tomasi, M. Cossi, N. Rega, N. J. Millam, M. Klene, J. E. Knox, J. B. Cross, V. Bakken, C. Adamo, J. Jaramillo, R. Gomperts, R. E. Stratmann, O. Yazyev, A. J. Austin, R. Cammi, C. Pomelli, J. W. Ochterski, R. L. Martin, K. Morokuma, V. G. Zakrzewski, G. A. Voth, P. Salvador, J. J. Dannenberg, S. Dapprich, A. D. Daniels, Ö. Farkas, J. B. Foresman, J. V. Ortiz, J. Cioslowski and D. J. Fox, *Gaussian 09 Revision D.01*, Gaussian, Inc., Wallingford, CT, USA, 2009.
15. A. E. Reed, J. E. Carpenter and F. Weinholf, *NBO version 3.1*, 1998.
16. R. F. W. Bader, *Atoms in Molecules: A Quantum Theory*, Oxford University Press, 1990.

17. T. Lu and F. W. Chen, *J. Comput. Chem.*, 2012, **33**, 580-592.
18. J. M. Wang, R. M. Wolf, J. W. Caldwell, P. A. Kollman and D. A. Case, *J. Comput. Chem.*, 2004, **25**, 1157-1174.
19. G. Schaftenaar and J. H. Noordik, *J. Comput. Aided Mol. Des.*, 2000, **14**, 123-134.
20. W. Humphrey, A. Dalke and K. Schulten, *J. Mol. Graphics Modell.*, 1996, **14**, 33-38.
21. M. Mercy, S. F. R. Taylor, J. Jacquemin, C. Hardacre, R. G. Bell and N. H. De Leeuw, *PCCP*, 2015, **17**, 28674-28682.
22. S. Seo, M. Quiroz-Guzman, M. A. DeSilva, T. B. Lee, Y. Huang, B. F. Goodrich, W. F. Schneider and J. F. Brennecke, *J. Phys. Chem. B*, 2014, **118**, 5740-5751.